Acta Cryst. (1980). B36, 416–421

The Three-Dimensional Structure of α-Amylase from Porcine Pancreas at 5 Å Resolution – The Active-Site Location

BY F. PAYAN, R. HASER, M. PIERROT, M. FREY AND J. P. ASTIER

Centre de Recherche sur les Mécanismes de la Croissance Cristalline, CNRS, Centre Scientifique de Saint-Jérôme, 13397 *Marseille CEDEX* 4, *France*

B. ABADIE

Institut de Chimie Biologique, 3 *place Victor Hugo,* 13331 *Marseille CEDEX* 3, *France*

AND E. DUÉE AND G. BUISSON

Département de Recherche Fondamentale, Centre d'Etudes Nucléaires, 85*X,* 38041 *Grenoble CEDEX, France*

(*Received* 16 *July* 1979; *accepted* 5 *November* 1979)

Abstract

The crystal structure of α-amylase from porcine pancreas (form I) has been established at 5 Å resolution. Form (I) crystallizes in space group $P2_12_12_1$ with $a = 56{\cdot}3$, $b = 87{\cdot}8$, $c = 103{\cdot}4$ Å, $Z = 1$ ($M_r = 53\,000 \pm 1000$). Three isomorphous derivatives have been used to solve the structure. The low-resolution electron-density map reported here provides information on: the overall architecture of the molecule; the labelling of the active centre with a modified maltotriose molecule; the identification of a second binding site for this substrate analogue, on the surface of the molecule; the location of the thiol groups and of one Ca^{2+} ion binding site in the α-amylase molecule.

Introduction

Several α-amylases (α-1,4-glucan-4-glucanohydrolase; EC 3.2.1.1) have been isolated and characterized from various sources. In mammals, pancreas α-amylase was purified from: hog (Marchis-Mouren & Pasero, 1967), rat (Vandermeers & Christophe, 1968), rabbit (Malacinski & Rutter, 1969), sheep (Ettalibi, Ben Abdeljii & Marchis-Mouren, 1975), and mouse (Danielsson, Marklund & Stijbrand, 1975); α-amylase was also purified from human saliva (Stiefel & Keller, 1973).

The enzyme hydrolyses long polyglucan chains according to a multiple-attack scheme (Robyt & French, 1970*a*). The results obtained with radioactive maltodextrines are consistent with a five glucose binding site in which the catalytic groups are located at bond 2 (Robyt & French, 1970*b*).

Porcine pancreatic amylase is a metalloprotein having one Ca^{2+} ion per molecule firmly bound and essential for enzymic activity (Vallée, Stein, Sumerwell & Fischer, 1959). The enzyme is also known to be activated by Cl^- ions (Levitzki & Steer, 1974). It exists as two equally active forms (I and II) which have the same molecular weight ($M_r = 53\,000 \pm 1000$) and amino-acid composition, but distinct isoelectric points (5·95 and 5·25 respectively). The molecule appears as a single N-acetylated polypeptide chain with, in particular, two thiol groups, four disulphide bridges and eight methionines (Cozzone, Pasero, Beaupoil & Marchis-Mouren, 1970). Nine peptides were isolated by cleavage of the chain with cyanogen bromide and were ordered further by means of a pulse-labelling technique (Cozzone & Marchis-Mouren, 1972). The sequences of some of the CNBr peptides were established, and the disulphide bridges as well as the two –SH groups were located. Very recently a partial amino-acid sequence has been determined (Pasero *et al.*, 1979). We report here the determination of the structure of porcine pancreatic α-amylase, form (I), at 5 Å resolution.

Experimental

(*a*) *Crystals*

Crystals suitable for X-ray diffraction could only be grown for porcine pancreatic α-amylase (McPherson & Rich, 1972) and for *Aspergillus oryzae* α-amylase (Kakudo, Kusunoki, Date, Matsuura & Tanaka, 1978). Meanwhile, several crystalline forms of porcine α-amylase could be isolated (Pierrot, Astier, Abadie & Marchis-Mouren, 1977; Haser, Payan, Pierrot, Buisson

0567-7408/80/020416-06$01.00

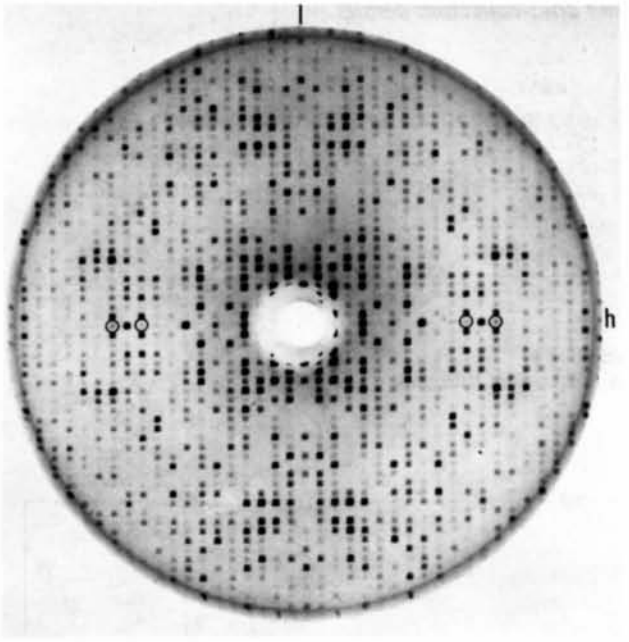

Fig. 1. Precession photograph of the *h0l* reciprocal-lattice plane of an α-amylase crystal. Reflections violating the 2_1 symmetry are circled. (Precession angle 16°; Cu $K\alpha$ radiation; exposure time 40 h; crystal–film distance 100 mm.)

& Duée, 1979). The most interesting form for further structure determination was the orthorhombic variety with one molecule per asymmetric unit, space group $P2_12_12_1$, with $a = 56{\cdot}3$, $b = 87{\cdot}8$, $c = 103{\cdot}4$ Å. Some odd-numbered reflections of the *h*00 class are observed at medium resolution [for instance, reflections {1100} and {1300} (Fig. 1)]. As no deviation from orthorhombic symmetry could be found one should conclude that the true space group is $P22_12_1$. However, this symmetry is not consistent with the difference-Patterson maps of the heavy-atom derivatives, whereas they were interpretable in space group $P2_12_12_1$. Therefore, the structure determination at low resolution was undertaken on the basis of $P2_12_12_1$ symmetry.

(*b*) *Heavy-atom derivatives and the protein–substrate analogue complex*

Steer & Levitzki (1973) showed that mercuration of the –SH groups could lead to amylase–$(SHg)_2$ or amylase–S–Hg–S potential derivatives for X-ray structural work; indeed, we found that the bridged S–Hg–S and $(SHg)_2$ derivatives crystallize isomorphously with the native enzyme. Other mercury derivatives were also prepared by the usual soaking techniques. Table 1 summarizes some details for the heavy-atom derivatives. It shows also that replacement of Ca^{2+} ions in α-amylase crystals by Ba^{2+} or Sr^{2+} was

Table 1. *Preparation conditions of the heavy-atom derivatives*

Derivative		Cocrystallization	
Amylase–S–Hg–S		(Steer & Levitzki, 1973)	
		Soaking conditions	
PAMA*		1 m*M*	10 d
$Pb(CH_3COO)_2$		10 m*M*	1 d
EMP†		1 m*M*	40 h
$Er(NO_3)_3$		2 m*M*	10 d
$LaCl_3$		4 m*M*	1 d
$SmCl_3$		4 m*M*	1 d
$YbCl_3$		4 m*M*	1 d
	Dialysis *versus*		
Ba^{2+}	$BaCl_2$	2 m*M*	3 d
Sr^{2+}	$SrCl_2$	2 m*M*	3 d

* PAMA = (*p*-acetylaminophenyl)mercury acetate.
† EMP = ethylmercury phosphate.

performed through dialysis *versus* $BaCl_2$ or $SrCl_2$. The interactions of some lanthanide ions with the enzyme were also observed by soaking crystals in solutions of $Er(NO_3)_3$, $LaCl_3$, $SmCl_3$ or $YbCl_3$. Another derivative, which proved very helpful, was obtained with $Pb(CH_3COO)_2$.

A substrate analogue was prepared and kindly supplied by H. Driguez (CERMAV, Grenoble). It is maltotriose modified as shown in Fig. 2. A native crystal was exposed for 10 h to a solution containing 7·5 m*M* of this compound. Successful binding was suggested by intensity changes observed on precession photographs.

(*c*) *Data collection and processing*

Intensities were collected on an Enraf–Nonius CAD-4 diffractometer with Ni-filtered Cu $K\alpha$ radiation. For each data set one single crystal approximately 0·5 × 0·35 × 0·5 mm was used to collect symmetry- and Friedel-related reflections (hkl, $\bar{h}kl$, $\bar{h}\bar{k}\bar{l}$). The crystal-to-detector distance was 368 mm and to reduce background scattering of air a helium-filled tube was interposed between the crystal and the detector. The diffractometer was operated in the ω scanning mode, the scanning time per reflection being around 60 s.

Crystal deterioration was monitored by measuring a standard set of six reflections at intervals. These reference intensities had dropped about 15–20% at the

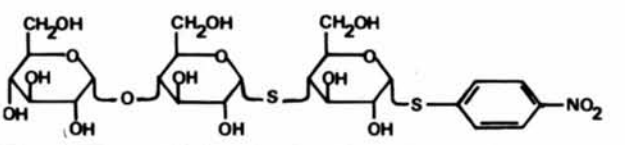

Fig. 2. The modified maltotriose [synthesized by H. Driguez (CERMAV, Grenoble)] used as substrate analogue.

Table 2. *Cell parameters and data-collection details*

	a (Å)	b (Å)	c (Å)	Data collected to	R_{SYM}	R_{FRI}
Native	56·3 (0·1)	87·8 (0·1)	103·4 (0·15)	4·7 Å	0·04	0·04
S–Hg–S	56·2	87·9	103·7	3·7	0·036	0·05
PAMA	55·9	87·4	103·0	5	0·032	0·10
$Pb(CH_3COO)_2$	56·1	87·8	103·2	5	0·030	0·10

$$R_{SYM} = \frac{\sum_h \sum_{l=1}^{N} |I(h)_l - \bar{I}(h)_l|}{\sum_h \sum_{l=1}^{N} I(h)_l}; \quad R_{FRI} = \frac{\sum ||F^+| - |F^-||}{\sum |F|}; \quad |F| = (|F^+| + |F^-|)/2.$$

$I(h)_l$ = lth intensity of reflection h.
$\bar{I}(h)_l$ = mean value of the N equivalent reflections.

end of data collection, except for the S–Hg–S derivative which appeared much less sensitive to radiation damage. The usual Lorentz and polarization corrections were made. Intensities were corrected individually for time-dependent decay by a radiation-damage function. The agreement indices between equivalent intensities, Friedel-related reflections and other pertinent data are listed in Table 2. Heavy-atom positions were deduced from the isomorphous difference-Patterson maps and further confirmed with cross-difference Fourier syntheses (Dickerson, Kopka, Varnum & Weinzierl, 1967). Positional and isotropic temperature parameters were refined by both F_{HLE} and 'lack of closure' refinements (Dodson & Vijayan, 1971; Dickerson, Kendrew & Strandberg, 1961). Difference syntheses were calculated based on coefficients $m(F_{PH} - F_P) \exp i\alpha_{Iso}$ where m is the figure of merit associated with phase α_{Iso} and F_{PH} and F_P are the structure factor amplitudes for protein plus heavy atom or substrate analogue and protein respectively. The phases were estimated by the method of Blow & Crick (1959).

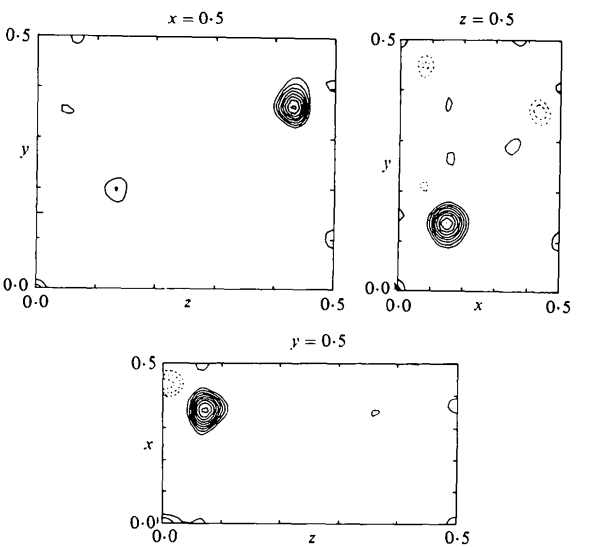

Fig. 3. The three Harker sections of the difference-Patterson function at 5 Å resolution for the amylase–S–Hg–S derivative, showing the unique Hg site. The contour levels are on an arbitrary scale.

(*d*) *Heavy-atom positions*

The difference-Patterson map for the bridged S–Hg–S derivative revealed one single binding site per molecule. Other mercury derivatives [EMP, PAMA, $-(SHg)_2$] yield the same solution to the difference map. Nevertheless, the PAMA derivative was used for phasing in view of its somewhat higher occupancy. The Pb derivative was interpretable in terms of three binding sites, none of them being common with the Hg site. Figs. 3 and 4 give the relevant Harker sections for both S–Hg–S and Pb derivatives. Many other potential derivatives gave difference-Patterson syntheses which were uninterpretable. However, when approximate protein phases were available, the difference maps showed clearly a common major binding site for the $BaCl_2$, $SrCl_2$, $LaCl_3$, $SmCl_3$ and $YbCl_3$ derivatives. These were not used for further phase determination

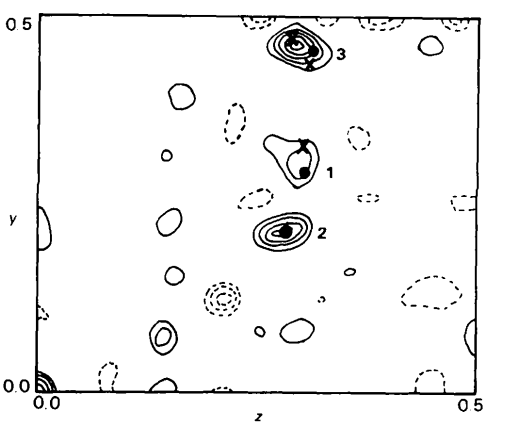

Fig. 4. Pb acetate derivative: Harker section at $u = a/2$. The black dots and the numbers refer to the sites of Fig. 6. Cross-vectors lying near the Harker plane are indicated by crosses.

Table 3. *Results of the refinement of the heavy-atom parameters at 5 Å resolution*

Derivative	Number of sites	Occupancy	x	y	z	B (Å^2)	R_F	R_{FHLE}	R_K	E/f
S–Hg–S	1	0·568	−0·1738 (7)	0·5674 (8)	0·2853 (5)	83	0·145	0·45	0·050	0·38
PAMA	1	0·594	−0·1741 (8)	0·5689 (6)	0·2834 (5)	115	0·150	0·47	0·083	0·65
$Pb(CH_3COO)_2$	3	0·428	−0·0665 (8)	0·3959 (5)	0·1508 (4)	56	0·154	0·44	0·046	0·39
		0·371	−0·0893 (9)	0·6396 (7)	0·1397 (6)	133				
		0·244	0·0306 (9)	0·5273 (7)	0·1570 (6)	130				

$$R_F = \frac{\sum||F_{PH}| - |F_P||}{\sum|F_P|}\,;\; R_{FHLE} = \frac{\sum|F_{HLE} - F_H|}{\sum F_{HLE}}\,;\; R_K = \frac{\sum|F_{PH}(\text{obs.}) - F_{PH}(\text{calc.})|}{\sum F_{PH}(\text{obs.})}\,.$$

$E/f = [\sum(|F_{PH}| - |F_P + F_H|)^2/n]^{1/2}/[\sum F_H^2/n]^{1/2}$; F_H = calculated heavy-atom contribution; n = number of reflections.

but they later proved essential in locating the Ca^{2+} ion of the α-amylase molecule. Table 3 summarizes some results of the refinement of the three heavy-atom derivatives. The final overall figure of merit for the 1700 independent reflections was 0·71.

Results

The electron-density map looks very clear and presents a high contrast between molecular and solvent regions. Only a few cuts at low electron-density levels were required to separate a molecule from its neighbours. The dimensions of the three major axes of the molecule are approximately 75, 55 and 50 Å.

The active site

The most striking feature at this resolution is the deep cleft (Fig. 5) which runs for 30 Å on one side of the molecule and separates two globular units which are very different in size. The molecular packing provides an important empty region next to the crevice allowing easy accessibility. The active site of α-amylase was immediately thought to be situated along this characteristic groove. Our preliminary substrate binding studies already confirmed this location: we considered first the interaction of the enzyme with a modified maltotriose molecule (Fig. 2), the replacement of the O atom of one α-1,4 bond by a S atom probably preventing the substrate analogue from complete hydrolysis.

The difference synthesis for the amylase-modified maltotriose complex showed two prominent, highly significant peaks (Fig. 6) which were assigned to two specific binding sites per protein molecule: one is deeply situated in the characteristic groove, the active-site region; the other is located on the surface of the molecule. The size of the two corresponding densities in the difference map suggested that this substrate

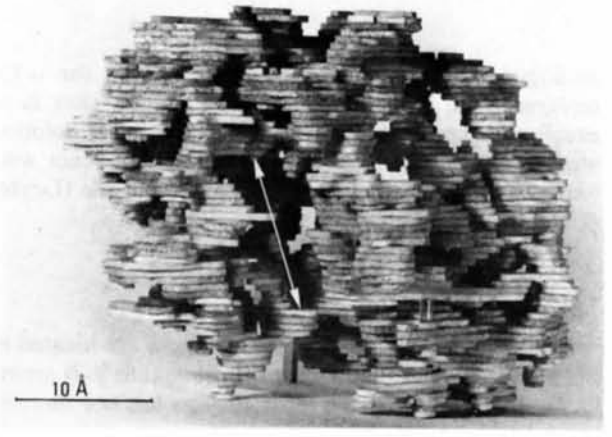

Fig. 5. A balsa-wood model of the α-amylase molecule. The active site is located in the crevice indicated by the long white arrow.

Fig. 6. A composite representation ($0·150 \leq z \leq 0·200$) of the native electron density and of the difference synthesis (hatched areas) for the maltotriose substrate. See text for the Pb sites. The two binding sites are about 20 Å apart.

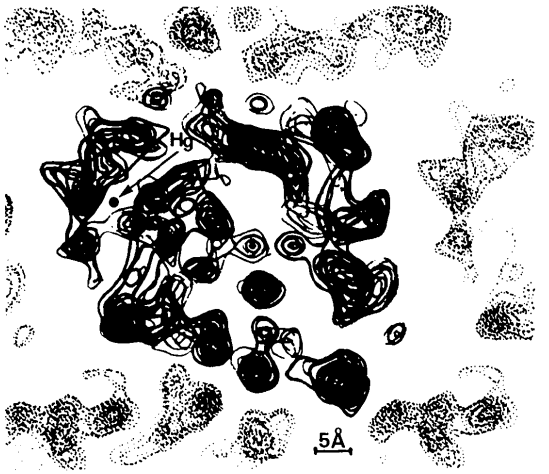

Fig. 7. The electron-density map around the Hg site ($0{\cdot}250 \leq z \leq 0{\cdot}300$).

analogue was most probably hydrolysed at the α-1,4 oxygen bond. The finding of two binding sites is in excellent agreement with the deductions from solution studies where maltotriose was observed to react with two specific regions of the α-amylase molecule (Loyter & Schramm, 1966).

The thiol groups

In Fig. 7 one can see that the Hg site is not located in the active site, but in a sort of tunnel next to it. It seems likely, therefore, that the –SH groups are not directly involved in the enzymic activity. Moreover, the present model indicates that a long continuous column of electron density runs close to the Hg site and ends in its vicinity. This observation is consistent with preliminary sequence studies demonstrating that one –SH group is close to the N terminal of the polypeptide chain (Cozzone & Marchis-Mouren, 1972).

The calcium sites

One essential Ca^{2+} ion is known to be strongly bound to the enzyme with a binding constant of $2 \times 10^{11}\ M^{-1}$ (Vallée *et al.*, 1959; Levitzki & Steer, 1974). This ion plays a key structural role in the stabilization of the enzyme: when it is removed by exhaustive dialysis *versus* EDTA solutions, α-amylase loses its activity. Addition of Ca^{2+} ions restores the activity (Steer & Levitzki, 1973). However, it is not clear whether this implies that Ca^{2+} takes part in the catalytic mechanism or merely that this ion ensures the correct tertiary structure required for activity.

In the presence of EDTA the structure is somewhat disturbed as the two –SH groups become exposed and, furthermore, reactive to bulky sulphydryl reagents like DTNB, while these groups are masked in the absence of EDTA (Schramm, 1964; Telegdi & Straub, 1973; Pommier, Cozzone & Marchis-Mouren, 1974; Steer, Tal & Levitzki, 1974).

When the three Pb sites were reported on the electron-density map (Fig. 6) it became clear that while Pb_1 and Pb_3 sites are in solvent regions close to the molecular surface, the Pb_2 site was superimposed on a strong density which could later be identified with an interchangeable Ca^{2+} ion.

This was confirmed by the analysis of the difference maps calculated for the Ba, Sr, and Sm derivatives, all of them indicating the same single substitution site ($x = -0{\cdot}089$, $y = 0{\cdot}640$, $z = 0{\cdot}140$). The Pb and Sm derivatives were prepared by soaking native crystals in solutions containing both Ca^{2+} ions and heavy-atom salts. This observation supports the idea that Ca^{2+} at the Pb_2 site is weakly bound to the protein since it can be replaced by another ion even in the presence of Ca^{2+} in the solution. It is clear, therefore, that this site is not related to the essential Ca^{2+} ion cofactor. The Sr and Ba derivatives prepared by dialysis also gave the same unique substitution. These results strongly suggest that porcine pancreatic α-amylase has two Ca^{2+} binding sites, one with a high affinity for the protein, the other easily interchangeable with other metals. At the present stage of the analysis the location of the strongly bound Ca^{2+} is still not clear and must await further work at higher resolution. Analysis of the crystal structure of α-amylase at 3 Å resolution and extension of the substrate binding studies are in progress.

Considering the different origins of the two enzymes, the comparison of the structures of porcine pancreatic and *A. oryzae* α-amylase (Kakudo *et al.*, 1978) should be very informative on the mechanism of action of α-amylases in general.

We are grateful to L. Sieker for helpful comments.

References

BLOW, D. M. & CRICK, F. H. C. (1959). *Acta Cryst.* **12**, 794–802.

COZZONE, P. & MARCHIS-MOUREN, G. (1972). *Biochim. Biophys. Acta*, **257**, 222–229.

COZZONE, P., PASERO, L., BEAUPOIL, B. & MARCHIS-MOUREN, G. (1970). *Biochim. Biophys. Acta*, **207**, 490–504.

DANIELSSON, A., MARKLUND, S. & STIJBRAND, T. (1975). *Int. J. Biochem.* **6**, 585–589.

DICKERSON, R. E., KENDREW, J. C. & STRANDBERG, B. E. (1961). *Acta Cryst.* **14**, 1188–1193.

DICKERSON, R. E., KOPKA, M. L., VARNUM, J. L. & WEINZIERL, J. E. (1967). *Acta Cryst.* **23**, 511–516.

DODSON, E. J. & VIJAYAN, M. (1971). *Acta Cryst.* **B27**, 2402–2411.

ETTALIBI, N., BEN ABDELJII, A. & MARCHIS-MOUREN, G. (1975). *Biochimie*, **9**, 995–999.

HASER, R., PAYAN, F., PIERROT, M., BUISSON, G. & DUÉE, E. (1979). *J. Chim. Phys.* **76**, 823–825.
KAKUDO, M., KUSUNOKI, M., DATE, W., MATSUURA, Y. & TANAKA, N. (1978). *Acta Cryst.* A**34**, S65.
LEVITZKI, A. & STEER, M. L. (1974). *Eur. J. Biochem.* **41**, 171–180.
LOYTER, A. & SCHRAMM, M. (1966). *J. Biol. Chem.* **241**, 2611–2617.
MCPHERSON, A. & RICH, A. (1972). *Biochim. Biophys. Acta*, **285**, 493–497.
MALACINSKI, G. M. & RUTTER, W. J. (1969). *Biochemistry*, **8**, 4382–4390.
MARCHIS-MOUREN, G. & PASERO, L. (1967). *Biochim. Biophys. Acta*, **140**, 366–368.
PASERO, L., ABADIE, B., MAZZEI, Y., MOINIER, D., BIZZOZERO, J. P., FOUGEREAU, M. & MARCHIS-MOUREN, G. (1979). *Ann. Biol. Anim. Biochim. Biophys.* **19**(4A), 1033–1041.
PIERROT, M., ASTIER, J. P., ABADIE, B. & MARCHIS-MOUREN, G. (1977). *FEBS Lett.* **79**, 105–108.
POMMIER, G., COZZONE, P. & MARCHIS-MOUREN, G. (1974). *Biochim. Biophys. Acta*, **350**, 71–83.
ROBYT, J. F. & FRENCH, D. (1970*a*). *Arch. Biochem. Biophys.* **138**, 662–670.
ROBYT, J. F. & FRENCH, D. (1970*b*). *J. Biol. Chem.* **245**, 3917–3927.
SCHRAMM, M. (1964). *Biochemistry*, **3**, 1231–1234.
STEER, M. L. & LEVITZKI, A. (1973). *FEBS Lett.* **31**, 89–92.
STEER, M. L., TAL, N. & LEVITZKI, A. (1974). *Biochim. Biophys. Acta*, **334**, 389–397.
STIEFEL, D. J. & KELLER, P. J. (1973). *Biochim. Biophys. Acta*, **302**, 345–361.
TELEGDI, M. & STRAUB, F. B. (1973). *Biochim. Biophys. Acta*, **321**, 210–219.
VALLÉE, B. L., STEIN, E. A., SUMERWELL, W. N. & FISCHER, E. H. (1959). *J. Biol. Chem.* **234**, 2901–2929.
VANDERMEERS, A. & CHRISTOPHE, J. (1968). *Biochim. Biophys. Acta*, **154**, 110–129.

Acta Cryst. (1980). B**36**, 421–424

The Structure of 1,1,3,5,7,7-Hexachloroheptane

BY J. C. J. BART*

Montedison Research Laboratories, Via S. Pietro 50, 20021 *Bollate, Milano, Italy*

AND I. W. BASSI AND M. CALCATERRA

Montedison 'G. Donegani' Research Laboratories, Via G. Fauser 4, *Novara, Italy*

(*Received* 7 *February* 1979; *accepted* 2 *October* 1979)

Abstract

The structure of a monoclinic modification of 1,1,3,5,7,7-hexachloroheptane, $C_7H_{10}Cl_6$, has been determined by X-ray diffraction techniques (911 observed reflections collected by an automatic diffractometer; final R value 0·043). Crystal data are: $C2/c$, $a = 12{\cdot}599$ (9), $b = 10{\cdot}320$ (6), $c = 9{\cdot}994$ (8) Å, $\beta = 107{\cdot}02$ (5)°, $Z = 4$. The molecule adopts staggered conformations throughout and is composed of a planar carbon skeleton. The two asymmetric C atoms of the molecule have the same configuration. Strain is relieved by considerable angular deformations. Chlorine bonds to di- and mono-substituted C atoms differ significantly, namely 1·772 (7) (average) and 1·802 (4) Å, respectively.

Introduction

In a recent paper (Bart, Bassi & Calcaterra, 1979) evidence has been given for a genuine effect concerning the C—Cl bond lengths in polychloro-substituted paraffins. In order to substantiate further the observed bond-shortening effects due to electronegative substituents we have now subjected 1,1,3,5,7,7-hexachloroheptane, (I), to an X-ray crystal structure determination. The product, which is an intermediate in the synthesis of flame retardants, had originally been obtained by telomerization of vinyl chloride and chloroform in the presence of ferrous chloride (Razuvaev, Bobinova, Zvezdin & Egorochkin, 1970).

Experimental

1,1,3,5,7,7-Hexachloroheptane crystallizes in at least two polymorphic modifications (orthorhombic and

* Present address: Montedison 'G. Donegani' Research Laboratories, Via G. Fauser 4, Novara, Italy.

0567-7408/80/020421-04$01.00